NASA Technical Memorandum 82763

The Use of Optimization Techniques to Design Controlled Diffusion Compressor Blading

(NASA-TM-82763) THE USE OF OPTIMIZATION TECHNIQUES TO DESIGN CONTROLLED DIFFUSION COMPRESSOR BLADING (NASA) 18 p
HC A02/MF A01 CSCL 21E N82-14094
Unclas
G3/07 08653

Nelson L. Sanger
Lewis Research Center
Cleveland, Ohio

Prepared for the
Twenty-seventh Annual International Gas Turbine Conference
sponsored by the American Society of Mechanical Engineers
London, England, April 18-22, 1982

NASA

NASA Technical Memorandum 82763

The Use of Optimization Techniques to Design Controlled Diffusion Compressor Blading

(NASA-TM-82763) THE USE OF OPTIMIZATICN TECHNIQUES TO DESIGN CONTRCLLED DIFFUSION COMPRESSOR BLADING (NASA) 18 p
HC A02/MF A01 CSCL 21E

N82-14094

Unclas
G3/07 08653

Nelson L. Sanger
Lewis Research Center
Cleveland, Ohio

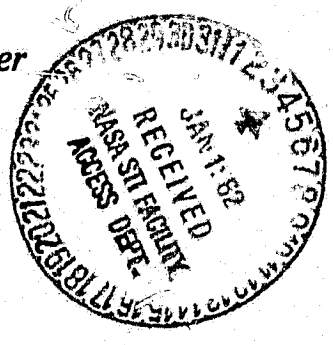

Prepared for the
Twenty-seventh Annual International Gas Turbine Conference
sponsored by the American Society of Mechanical Engineers
London, England, April 18-22, 1982

NASA

THE USE OF OPTIMIZATION TECHNIQUES TO DESIGN CONTROLLED DIFFUSION COMPRESSOR BLADING

by Nelson L. Sanger*

National Aeronautics and Space Administration
Lewis Research Center
Cleveland, Ohio 44135

ABSTRACT

A method is presented for automating compressor blade design using numerical optimization, and is applied to the design of a controlled diffusion stator blade row. A general purpose optimization procedure is employed, which is based on conjugate directions for locally unconstrained problems and on feasible directions for locally constrained problems. Coupled to the optimizer is an analysis package consisting of three analysis programs which calculate blade geometry, inviscid flow, and blade surface boundary layers.

The optimization concepts are briefly discussed. Selection of design objective and constraints is described. The procedure for automating the design of a two-dimensional blade section is discussed, and design results are presented.

*Member ASME.

THE USE OF OPTIMIZATION TECHNIQUES TO DESIGN CONTROLLED DIFFUSION COMPRESSOR BLADING

by Nelson L. Sanger*

National Aeronautics and Space Administration
Lewis Research Center
Cleveland, Ohio 44135

ABSTRACT

A method is presented for automating compressor blade design using numerical optimization, and is applied to the design of a controlled diffusion stator blade row. A general purpose optimization procedure is employed, which is based on conjugate directions for locally unconstrained problems and on feasible directions for locally constrained problems. Coupled to the optimizer is an analysis package consisting of three analysis programs which calculate blade geometry, inviscid flow, and blade surface boundary layers.

The optimization concepts are briefly discussed. Selection of design objective and constraints is described. The procedure for automating the design of a two-dimensional blade section is discussed, and design results are presented.

*Member ASME.

THE USE OF OPTIMIZATION TECHNIQUES TO DESIGN CONTROLLED DIFFUSION COMPRESSOR BLADING

by Nelson L. Sanger*

National Aeronautics and Space Administration
Lewis Research Center
Cleveland, Ohio 44135

E-1084

NOMENCLATURE

AC1,BC1,CC1,DC1, AC2,BC2,CC2,DC2	polynomial coefficients for blade angle distribution expression
AT1,BT1,CT1,DT1 AT2,BT2,CT2,DT2	polynomial coefficients for blade thickness distribution expression
C	chord
$F(\bar{X})$	objective function
$G_j(\bar{X})$	constraint functions
Hi	incompressible form factor
$H_{i,crit}$	critical value of incompressible form factor at which turbulent boundary layer separates. $H_{i,crit} = 2.0$ in this study
L.E.	leading edge of blade
KCS	angle with respect to meridional direction of blade mean line midway between transition location and trailing edge
KICR	angle with respect to meridional direction of blade mean line at leading edge
KOCR	angle with respect to meridional direction of blade mean line at trailing edge
KTC	angle with respect to meridional direction of blade mean line at transition location
$\bar{S}$	search direction
s_1	distance from transition location along mean line, front segment
s_2	distance from transition location along mean line, rear segment
s_{m1}	distance from maximum thickness location along mean line, front segment
s_{m1e}	distance from maximum thickness location to blade leading edge along mean line
s_{m2}	distance from maximum thickness location along mean line, rear segment
s_{m2e}	distance from maximum thickness location to blade trailing edge along mean line
T	distance from leading edge to intersection of two polynomial segments describing mean line/chord
t_1, t_2	thickness of blade, front and rear segments respectively
TMX	maximum thickness/chord
T.E.	trailing edge
U	stream function
V	surface velocity
$\bar{X}$	vector of design variables
XCHORD	meridional projection of blade chord
ZM	distance from leading edge to maximum thickness location/chord
α^*	move parameter
κ	blade angle

Subscripts:

1	front segment
2	rear segment
m	number of constraints
n	number of design variables
ps	pressure surface
ss	suction surface
t	transition

*Member ASME.

INTRODUCTION

Throughout the history of compressor technology, blade shapes have been specified by geometric families or classes. For the most part, these families have been derived from early wing shapes and improved by empiricism, or have been directly specified from simple geometric shapes such as circular arcs and parabolas.

During the past decade, computational methods for the calculation of flow through compressor blade rows have advanced substantially, as have computer speeds. With these advances has come the capability to rapidly design and analyze flow over arbitrary blade shapes. Indeed, at the present time, these analysis methods are being synthesized into computer-aided design systems. In most cases these systems are "manual", i.e., non-automated. Because of the great flexibility in choice of blade shape, the design process can become quite cumbersome and repetitive unless automated in some fashion. One of the most attractive methods for automating the design process is numerical optimization. Much progress has been made recently in bringing the technique to bear on engineering problems, particularly in the field of Aeronautics (1). Of the many numerical optimization algorithms in existence, the one used in Ref. 1 and described in Ref. 2 with its control program (3) is sufficiently general and user-oriented to be of particular interest. It is used in the work reported herein, and is coupled to analysis programs which calculate blade shape, the inviscid flow field, and the boundary layer for a two-dimensional blade section.

With the advent of arbitrary blade shapes, the concept of controlling velocity diffusion (and consequently boundary layer growth) on the suction surface has received increasing attention. In the transonic flow regime, such blading has generally been referred to as "supercritical blading" since the local supersonic flow is controlled as well as the boundary layer growth. In the subsonic regime the blading is often simply referred to as "controlled diffusion". Methods of analysis have generally been inverse, in which a velocity distribution of a general Stratford type (4) is prescribed at the outset, and a blade shape derived from it (5 and 6).

The problem addressed in the present work is the redesign of a high-subsonic stator blade row utilizing a controlled diffusion blade shape. The analytical methods are direct rather than inverse. A blade shape is initially prescribed and aerodynamic performance calculated. Perturbations on the blade shape are effected and aerodynamic performance recalculated until specified conditions are met. The resulting velocity distributions over the suction surface of the blade are also of the general Stratford type, but in this case are controlled by constraints imposed on the geometric and aerodynamic parameters.

The subject stator row uses the same flow path and velocity triangles as the first stage stator of the NASA Two-Stage Fan (7). The original design was highly successful, showing a first stage peak adiabatic efficiency of 87.0 percent, and a remarkably low radial distribution of loss across the stator. Consequently, significant improvement in performance with controlled diffusion blading cannot be expected, nor is that the purpose of the present work. The principal objective of the work presented herein is to develop and demonstrate the feasibility of an automated design procedure based on numerical optimization. Experimental evaluation of the resulting design is planned for both a single-stage environment and a two-dimensional cascade (midspan blade section).

ANALYSIS METHODS

Blade Section Geometry

The blade section geometry is generated by a polynomial element program. This program has been extracted from the NASA Design Program which is a streamline curvature design procedure (8). Blade section nomenclature is presented in Fig. 1. The meanline of the blade is described by two polynomial segments, each of which can be specified by up to a quartic polynomial. The polynomial is a fit of local mean-line blade angle against mean-line distance. The fraction of chord from the leading edge at which the two polynomial segments join is referred to as the transition location, T. The polynomials may be fitted beginning from the transition location and fitting toward the leading edge and trailing edge respectively, or they may be fitted beginning at the leading and trailing edges and fitting toward the transition location. In this report, fitting from transition location toward leading and trailing edges for each segment is the mode of operation. Note that s_1 and s_2 are both positive in this mode.

The expression for blade angle distribution is given by Eq. (1): front segment:

$$\kappa_1 = \kappa_t + AC1 \times s_1 + BC1 \times s_1^2 + CC1 \times s_1^3 + DC1 \times s_1^4 \qquad (1A)$$

Rear segment:

$$\kappa_2 = \kappa_t + AC2 \times s_2 + BC2 \times s_2^2 + CC2 \times s_2^3 + DC2 \times s_2^4 \qquad (1B)$$

A typical distribution of blade angle is shown in Fig. 2(a). The blade angle at the transition location is designated as KTC. When fitting from the transition location, the fit is effected from KTC to the blade angle at inlet, KICR (front segment), and from KTC to the blade angle at outlet, KOCR (rear segment). Noted on the figure is a parameter calculated internally by the program, KBS, which is the blade angle midway between the transition location and the trailing edge. This parameter will be of importance in later discussion.

The distribution of blade thickness about the mean-line is also specified by two polynomials, both of which may be quartics. The thickness is added symmetrically on either side of the meanline. The fit is made from the maximum thickness location toward the leading and trailing edges for front and rear segments respectively. The leading edge and trailing edge may be specified as circles or ellipses. Circles only were used in this design. The equations for thickness distribution are given as Eq. (2). Instead of being linear, the first term is of a square root form, which enables simulation of 65-series blades, if desired.

Front segment:

$$t_1 = \frac{TMX}{2} + AT1 \times \left(\sqrt{s_{m1e} - s_{m1}} - \sqrt{s_{m1e}} + \frac{s_{m1}}{2\sqrt{s_{m1e}}} \right) - BT1 \times s_{m1}^2 - CT1 \times s_{m1}^3 - DT1 \times s_{m1}^4 \qquad (2A)$$

Rear segment:

$$t_2 = \frac{TMX}{2} + AT2 \times \left(\sqrt{s_{m2e} - s_{m2}} - \sqrt{s_{m2e}} + \frac{s_{m2}}{2\sqrt{s_{m2e}}} \right) - BT2 \times s_{m2}^2 - CT2 \times s_{m2}^3 - DT2 \times s_{m2}^4 \qquad (2B)$$

Potential Flow Solution

The potential flow about the blade section in the two-dimensional, blade-to-blade plane is calculated by the method developed by Katsanis, TSONIC (9). The program solves the stream function equation by finite difference techniques for the subsonic, compressible flow regime. It is necessary to specify as input the fluid properties, inlet total temperature and density, weight flow, blade geometry, inlet and outlet flow angles, finite difference mesh, and a meridional distribution of streamtube height and total pressure loss. In the design presented herein, a linear distribution of streamtube height and estimated total loss was utilized.

Because the nature of the equations dictates that the solution be of a boundary value type, the outlet flow angle must be specified on the downstream boundary. This effectively sets the Kutta condition. Since this condition is related to one of the constraints chosen for the optimization process, its discussion will be reserved until later.

Boundary Layer Calculations

Blade surface boundary layers were calculated using the program developed by McNally (10). In addition to the surface velocities, required input includes upstream flow conditions, fluid properties, and blade surface geometry. Among the output provided by the program are the conventional boundary layer thicknesses, form factors, wall friction coefficient, and momentum thickness Reynolds number.

The program uses integral methods to solve the two-dimensional compressible laminar and turbulent boundary layer equations in an arbitrary pressure gradient. Cohen and Reshotko's method (11) is used for the laminar boundary layer, transition is predicted by the Schlicting-Ulrich-Granville method (12), and Sasman and Cresci's method (13) is used for the turbulent boundary layer.

A boundary layer which is initially laminar may proceed through normal transition to a turbulent boundary layer, or it may undergo some form of laminar separation before becoming turbulent. To provide flexibility for analyzing this behavior, several program options are available to the user. The calculations may proceed from a laminar boundary layer through transition to turbulent calculations. However, if laminar separation is predicted before transition, the turbulent calculations may be started by specifying a factor by which the last calculated value of momentum thickness is multiplied (this value is commonly chosen to be 1.0 to satisfy conservation of momentum). This new momentum thickness and a value for form factor based on the last calculated momentum thickness Reynolds number are used as initial values for the turbulent calculations.

Optimization Program

The optimization algorithm in Fortran code is known as CONMIN, and is reported in Ref. 2. A general purpose control program known as COPES is coupled to the algorithm (3).

The general mathematical representation of a numerical optimization problem is stated as:

$$\begin{aligned} &\text{Minimize} && OBJ = F(\bar{X}) \\ &\text{subject to} && G_j(\bar{X}) < 0. \qquad j = 1,m \\ & && X_i^{\ell} < X_i < X_i^{u} \qquad i = 1,n \end{aligned} \qquad (3)$$

$\bar{X}$ is a vector consisting of the design variables. X_i^{ℓ} and X_i^{u} are the lower and upper bounds on the design variables and are referred to as side constraints. OBJ is the objective function. If the designer wishes to maximize a function, OBJ may be defined as the negative of the function. $G_j(\bar{X})$ set the constraint functions which the design must satisfy. When $G_j(\bar{X}) < 0$, it is said to be inactive; when $G_j(\bar{X}) > 0$, it is violated. When it is within a tolerance band about zero, it is active. $F(\bar{X})$ and $G_j(\bar{X})$ may be implicit or explicit functions of the design variables $\bar{X}$, but must be continuous. (Note: this should be carefully considered when formulating these functions when they are calculated from finite difference solutions or at discrete stations.)

An initial design vector, $\bar{X}$, is specified by the user. It may be feasible or infeasible, i.e., if it satisfies the inequalities of Eq. (3), it is feasible. If a feasible initial design can be found, it is usually more efficient to begin with it, at least for the types of problems discussed herein. An iteration process is then begun which follows the recursive relationship:

$$\bar{X}^{q+1} = \bar{X}^{q} + \alpha^* \bar{S}^{q} \qquad (4)$$

q is the iteration number; the vector $\bar{S}$ is the search direction in the n-dimensional space; and the scalar α^* (move parameter) defines the distance of travel in direction $\bar{S}$, and is found by interpolation.

The search direction $\bar{S}$ is initially obtained by moving in the direction of steepest descent (negative gradient of the objective function) without violating constraints. The procedure is then repeated using a conjugate direction algorithm in determining a new search direction. Whenever a constraint is encountered, a new search direction is found using Zoutendijk's Method of Feasible Directions. An optimum has been achieved when no search direction can be found which will further reduce the objective function without violating a constraint.

OPTIMIZATION OF STATOR BLADE SECTION

Formulation of a specific optimization problem involves choice of an objective function (the quantity to be optimized), choice of constraints, and choice of design variables. In the present design problem, optimization of a two dimensional stator blade section was performed at the 90 percent span from tip section. This location represented the most difficult design problem as measured by blade loading requirements.

Results of preliminary calculations of an initial blade shape which meets the specified velocity triangles at the 90 percent span location are shown in Figs. 2 to 4. Figure 2 shows the distribution of blade angle and blade thickness along the mean-line, and the corresponding blade shape. Figure 3 is the surface velocity distribution corresponding to the blade shown in Fig. 2. And Fig. 4 represents the incompressible form factor distribution along the suction surface obtained from the boundary layer calculations.

The initial blade design was essentially an arbitrary choice. The blade angle distribution and thickness distribution plots were determined by running the blade geometry program in a graphics mode. In this mode, the distributions can be generated by curvefitting through points which are input by the user. The process is therefore intuitive, and guided by experience. The only restriction to the process is the desirability, with regard to optimization theory, that the design be feasible. Note that for the initial design selected, the turbulent boundary layer separates at 64 percent of chord.

A properly designed controlled diffusion blade should experience no suction surface boundary layer separation. This criterion is incorporated into the objective function. The following penalty function type of objective function proved to be the most successful.

$$OBJ = FORMAX - XSEPOX \qquad (5)$$

FORMAX is the maximum incompressible form factor (H_i) occuring over the rear portion of the blade, and XSEPOX is the separation location of the turbulent boundary layer expressed as a proportion of chord length.

OBJ was minimized. Reducing FORMAX acts to increase the separation location, XSEPOX. Simultaneously reducing FORMAX and increasing XSEPOX acts to reduce OBJ.

Design Variables

Nine design variables have been selected, all of which describe the geometry of the blade. These variables are:

T, transition location of two mean-line polynomials;
ZM, maximum thickness location;
KOCR, the exit blade mean-line angle (deg.);
AC1,BC1, first two coefficients of front segment mean-line polynomial;
AC2,BC2,CC2,DC2, all four coefficients of rear segment mean-line polynomial.

The velocity triangles are fixed for the blade section, thus fixing the loading or overall velocity diffusion across the blade row. By allowing KOCR to vary, the blade camber angle is allowed to change. The trailing edge or Kutta-type condition is controlled through a constraint described below.

Incidence angle is not allowed to vary. It is fixed at the value used in the original design (7) simply as a designer's preference. If it should become desirable or necessary to allow incidence angle to vary, it can easily be incorporated by including KICR as a design variable, and retaining the same velocity triangle information.

Although the maximum thickness location, ZM, is allowed to vary, the coefficients of the blade thickness polynomial are held fixed at the values used in the preliminary (initial) blade shape, strictly as a designer's choice.

Each of the above variables is allowed to vary within user-selected limits. The upper and lower bounds for each are listed below, and in optimization theory are referred to as side constraints. The side constraint values are chosen as a result of experience. Beyond certain values, a realistic blade shape will not result. In addition, certain extreme combinations of variables may cause convergence problems in the geometry program, and so are best avoided.

	Lower Bound	Upper Bound
Transition Location/Chord, T	.20	.40
Max Thickness Loc./Chord, ZM	.35	.55
Outlet Blade Angle, KOCR	-10.	-2.
All Coefficients	1.E-15	1.E+15

Constraints

Five constraint functions are specified, all being implicit functions of the design variables. Two constraints are variables calculated internally to the geometry program and control the blade angle distribution. By controlling the blade angle distribution, a controlled diffusion type shape to the surface velocity distribution can be insured. The constraints are represented in Fig. 2(a), and are KTC and KCS, which were previously described. They were allowed to vary between the following bounds:

	Lower Bound	Upper Bound
KTC	32.0	46.08
KCS	-4.0	11.05

The remaining constraints are calculated in the inviscid flow program (9) and are described with reference to a surface velocity distribution. Since TSONIC is principally a subsonic calculation procedure, the maximum surface velocity on the suction surface is constrained to the subsonic flow regime. A search procedure locates the maximum suction surface velocity. This is nondimensionalized by the inlet freestream velocity and the ratio is defined as the constraint. The upper bound was set to be equivalent to Mach 1 condition. The lower bound is set equal to an arbitrary, small number.

Because no boundary layer calculations are made on the pressure surface of the blade, a constraint is applied to control the velocity diffusion on the pressure surface. Preliminary calculations were made of typical blade shapes, and a pressure surface velocity diffusion (V,max/V,min) of 1.65 was deemed to be a sufficiently safe upper bound. Subsequent to the optimization calculation, the pressure surface boundary layer of the optimized blade is also calculated to verify that it was truly free from separation. The lower bound of this constraint is set equal to an arbitrary, small number.

The final constraint is chosen to set the trailing edge condition, the condition equivalent to a Kutta condition. This is also equivalent to setting deviation angle. In the present work, outlet flow angle is fixed, so whatever value is taken on by blade outlet angle, KOCR, sets deviation angle. Experience with some of the conventional families of blades, supplemented with detailed analyses, permitted guidelines to be set for estimating deviation for those blade families (14). But such experience is lacking for controlled diffusion blading, which is arbitrary in shape. For conventional blading, setting the deviation angle such that the suction surface and pressure surface velocity distributions close inside the trailing edge at perhaps 85 to 90 percent of chord, was one possible means for accounting for the effect of a rounded trailing edge and boundary layer separation over the rear portion of the suction surface. For controlled diffusion blading, the object is to have no boundary layer separation. If this is accomplished, the deviation angle would be expected to be small, and there would be justification for allowing the suction surface and pressure surface velocities to close at the trailing edge, rather than closing earlier.

The constraint is defined as a non-dimensional difference between velocities on the suction and pressure surfaces at the trailing edge mesh line, and is expressed:

$$\frac{(V_{ss} - V_{ps})_{T.E.}}{15.24} \qquad (6)$$

The denominator, 15.24, was chosen to scale the constraint to about order one. Upper bound was set at zero and lower bound at -1.25. The velocity difference at the trailing edge could vary between an upper bound of zero and a lower bound of -19.0 m/sec, thus permitting some closing inside the trailing edge.

MODIFICATIONS OF ANALYSIS PROGRAMS

An important requirement of the optimization method is that the objective and constraint functions be continuous functions of the design variables. This necessitated certain modifications of the analysis programs.

Modification of Inviscid Code

Experience with the TSONIC code has shown that calculations in the trailing edge region can be quite sensitive for some configurations. Orientation of the blade, trailing edge radius, and grid intersection points can affect surface velocity calculations at or near the trailing edge station, sometimes resulting in spurious behavior. Inaccurate trailing edge velocities will produce incorrect gradients of the trailing edge constraint described above, and possibly give misleading violations of that constraint.

The means used to avoid or reduce this tendency is to incorporate a mass injection model at the trailing edge (15). In this model, tangents are formed at the intersection of the trailing edge circle with the blade surface, and extended to the vertical grid line which forms a tangent with the trailing edge circle (Fig. 5). The "wake" is then extended downstream with an orientation determined by the downstream whirl boundary condition. Experience has shown this modeling to reduce the sensitivity of the surface velocity calculations in the trailing edge region.

Modifications of Boundary Layer Code

There is presently no agreement concerning the initial state of a boundary layer on a compressor stator blade in the real flow environment. Some observors have measured laminar boundary layers, while others contend that due to high inlet turbulence and unsteady effects, a laminar boundary layer cannot persist. For the purposes of this study, the question is somewhat academic. An optimization design process can be developed for either case. In the present work the existence of a laminar boundary layer is assumed, which poses the more difficult optimization problem.

The location of laminar separation and turbulent reattachment is of crucial importance to the optimization search process. The suction surface velocity distribution provided as input to the boundary layer calculation might ideally appear as represented in Fig. 6(a). In reality it might appear as in Figs. 6(b) and (c), due to the interrelationship of geometric variables such as blade stagger, solidity, camber distribution, thickness distribution, transition location, and maximum thickness location. Boundary layer calculations are initiated with a laminar boundary layer, which would usually persist to point A. Laminar separation, rather than normal transition, occurs there in all cases because of the steep adverse pressure gradient. Conservation of momentum is assumed through the laminar separation region, with the turbulent boundary layer reattached at the next calculating station. Turbulent separation is assumed to occur when the incompressible form factor reached a critical value.

As originally modelled, point A (Fig. 6) is identified as the station at which skin friction becomes negative. Any sensitivity to design variables can cause a discontinuous jump in point A location. This effect carries through to directly influence turbulent boundary layer separation location and the objective function. To establish a consistent and conservative criterion, the following procedure was coded. Using Lagrangian interpolation, three additional points are placed between each station in the high gradient region of the velocity vs. distance array. A search procedure is begun from the trailing edge region, and locates the maximum velocity at the beginning of the high gradient region, point B in Fig. 6. Laminar separation and turbulent reattachment is effected at point B.

In addition to the modifications discussed above, several modifications were required relating to turbulent boundary layer separation. A separation criterion common to compressor blade analyses which use integral boundary layer methods is the incompressible form factor, H_i. Values of 1.8 to 2.6 have been proposed and used in the past (e.g., von Doenhoff and Tetervin, Ref. 16). A value of 2.0 is somewhat conservative and, in the experience of the author, has proven to be useful. The program was modified to use 2.0 as the critical incompressible form factor.

In normal operation, when a form factor at a given station exceeds 2.0, separation is assumed to have occurred at that station. If calculation stations are 5 percent of chord apart, separation location becomes a discontinuous function, changing with distance in 5 percent jumps. To correct this,

linear interpolation is used between stations to obtain the percent chord location corresponding to $H_i = 2.0$.

Because of the relation between blade angle distribution and thickness distribution, the incompressible form factor quite often resembles Fig. 7. A maximum form factor can be observed at C. A more conventional form factor distribution is also depicted in Fig. 7, where the maximum value is identified as D. A search procedure was added to locate the maximum form factor, formax, which is one term in the objective function.

It was observed that allowing turbulent reattachment at a momentum thickness equivalent to momentum thickness at laminar separation often resulted in initial turbulent momentum thickness Reynolds numbers less than 320, the minimum value experimentally observed for a turbulent boundary layer (17). Therefore, as a final modification, the code was altered to provide a minimum thickness equivalent to a Reynolds number of 320.

DESIGN RESULTS

The optimization history is shown in Fig. 8. Most improvement occurred in the first two iterations. At the end of two iterations a blade had been found with no boundary layer separation (XSEPOX = 1.0). Reduction of the objective function for subsequent iterations involved reduction of FORMAX only, since XSEPOX remained 1.0. All improvement beyond iteration 2 provided more safety margin from the theoretical separation condition. CPU time on an IBM 370/3033 for the eight iterations was 49.48 minutes. A total of 85 calls on the analysis programs were made.

The initial and final blade shapes, surface velocities, and suction surface boundary layer form factor are presented and compared in Figs. 9 to 11. The pressure surface boundary layer form factor is presented in Fig. 12.

In the course of optimization, the geometric transition location moved forward from 27.3 percent of chord to 24.1, and the level of KTC (blade angle at transition) shifted downward from 36.7 degrees to 34.8 (Fig. 9). The maximum thickness location moved rearward from 48.2 percent of chord to 53.6. All polynomial coefficients describing the blade angle distribution were altered, as would be expected, since they were design variables. The polynomial coefficients describing the thickness distribution were not altered, since they were not design variables. However, since the maximum thickness location itself changed, the actual distribution of thickness was altered, as is evident from Fig. 9(b). If difficulties in achieving a satisfactory design had been experienced, the polynomial coefficients for thickness distribution could have been added as additional design variables, but at the cost of increased computing time. Outlet blade angle, KOCR, changed little during the process. Large excursions in KOCR were prevented because it is closely related to the trailing edge constraint (Eq. (6)).

The changes effected in the surface velocities by the optimization procedure (Fig. 10) are a bit more dramatic in appearance than are the geometry changes. The peak velocity on the suction surface was reduced, as was the large velocity diffusion over the front portion of the pressure surface. The unconventional waviness of the pressure surface velocity is due to the aft location of the maximum thickness. Fitting the thickness distribution through this maximum thickness location, in combination with the forward transition location, results in a region of reversed curvature on the pressure surface near the maximum thickness location, and is evident on Fig. 9(c). The effect on the flow carries across the channel and appears as a small wave on the suction surface as well. Aside from the dubious aesthetic appearance, no adverse aerodynamic effects can be attributed to this behavior. The calculated boundary layers appear well-behaved, with the maximum incompressible form factor on the suction surface being 1.924, and on the pressure surface 1.780.

In completing the design of the stator, only one other blade section was optimized, the hub section at the inner endwall. This blade element will be in the wall boundary layer, so that true two-dimensional flow is not expected to exist. Resulting transition location and maximum thickness location were not greatly different from the values found at the 90 percent span location. Blade angle polynomial coefficients different from those obtained at 90 percent span were obtained. However, for reasons relating to the blade stacking procedure, which will be described below, the polynomial coefficients obtained at the 90 percent span location were used also at the 100 percent span. The resulting two-dimensional calculations for the blade with these coefficients indicated no boundary layer separation.

All other blade sections were specified based on the optimized design obtained at the 90 percent span section. Each of these blade sections, which lie on streamlines, is then radially stacked. Fabrication coordinates are interpolated at several planes parallel to the axis of rotation of the compressor. In principle, each of the blade sections on the six chosen streamlines utilized could be designed by optimization. This could and probably would result in six different sets of transition location, maximum thickness location, and blade angle polynomial coefficients. The fabrication coordinates are generated by a design point streamline curvature code. As input to this code, a radial curvefit of each of the polynomial coefficients must be provided. Transition location and maximum thickness location for each blade section are input directly. The blade coordinates on each streamline section are then generated. Finally, coordinates at the horizontal fabrication planes are obtained by interpolation, based on a cubic fit of the blade coordinates at the four streamlines most closely straddling the desired fabrication plane.

Because of the curvefitting at various stages of this process, prudence suggests avoiding the possibility of large radial variations in the design parameters. Therefore, a constant radial distribution of each parameter was sought, with one exception. Maximum thickness location was arbitrarily moved forward to 47 percent of chord for all sections between the tip and 70 percent of span from tip. Although it was not necessary to do this, the effect was to relieve the reversed curvature condition on the pressure surface. The transition location and all polynomial coefficients were maintained at the same values obtained for the optimized 90 percent span section. At the 100 percent span section, transition and maximum thickness locations found from optimization at that section were used (0.26 and 0.52 respectively), and blade angle polynomial coefficients equivalent to those at 90 percent span were used. Thus, neither the polynomial coefficients for blade angle nor maximum thickness

varied radially. Transition location was constant from tip to 90 percent span, and differed only slightly at 100 percent span. Maximum thickness location was constant from the tip to 70 percent span at 0.47, moved rearward to 0.53 at 90 percent span, and slightly forward to 0.52 at 100 percent span. The exit blade angle, KOCR, varied only slightly from tip to hub in a range from -3.7 to -4.0. Since design exit flow angle is zero degrees for all sections, the negative value of KOCR represents deviation angle. If, indeed, the boundary layer does not separate from the blade as theoretically predicted, the deviation angles of about 4 degrees may be more realistic than they appear to be. The blade geometry and surface velocity distributions for the blade sections at midspan and 10 percent span from tip are shown in Figs. 13 and 14.

SUMMARY AND CONCLUDING REMARKS

A method has been presented for automated compressor blade design using numerical optimization techniques. The method was applied to the design of a controlled-diffusion stator blade row. Three analysis programs were coupled to the numerical optimization program: a blade geometry generation program which uses polynomial representation for blade angle and thickness distributions, a compressible, inviscid flow program, and an integral boundary layer program. Seven of the nine design variables were related to blade angle distribution, another located the maximum thickness of the blade, and the last controlled camber and deviation angles. Two constraint functions operated in the geometry program to produce shapes with controlled diffusion velocity distributions. Constraint functions applied in the flow analysis programs limited suction surface velocities to the subsonic regime, limited the velocity diffusion on the pressure surface, and set the trailing edge condition for inviscid calculations. The objective function, which was minimized, was of a penalty function form, and effectively produced a blade whose suction surface turbulent boundary layer did not separate.

The optimization procedure for the subject blade section required eight major iterations involving 85 calls on the geometry/aerodynamic analysis programs. Total CPU time on an IBM 370/3033 computer was 49.48 minutes.

When using the numerical optimization procedure, it was essential that the gradients of the constraint and objective functions be smooth and accurate. Therefore, some modifications of the analysis programs were necessary to ensure that these functions were continuous.

The design problem, as formulated here, produced a blade shape which satisfied the design criteria, while holding the polynomial coefficients describing thickness distribution, the value of maximum thickness, and the incidence angle constant. The method thus still offers great flexibility for adaptation to more demanding design requirements.

REFERENCES

1 Vanderplaats, G. N., "The Computer for Design and Optimization," Computing and Applied Mechanics, AMD-Vol. 18, American Society of Mechanical Engineers, New York, 1976, pp. 25-48.

2 Vanderplaats, G. N., "CONMIN a Fortran Program for Constrained Function Minimization, User's Manual," NASA TM X-62282, 1973.

3 Vanderplaats, G. N., "COPES a Fortran Control Program for Engineering Synthesis," Naval Postgraduate School, 1980.

4 Stratford, B. S., "The Prediction of Separation of the Turbulent Boundary Layer," Journal of Fluid Mechanics, Vol. 5, Pt. 1, Jan. 1959, pp. 1-16.

5 Papailiou, K. D., "Boundary Layer Optimization for the Design of High Turning Axial Flow Compressor Blades," ASME Paper No. 70-GT-88, 1970.

6 Stephens, H. E., "Application of Supercritical Airfoil Technology to Compressor Cascades: Comparison of Theoretical and Experimental Results," AIAA Paper No. 78-1138, July 1978.

7 Urasek, D. C., Gorrell, W. T., and Cunnan, W. S., "Performance of Two-Stage Fan Having Low-Aspect-Ratio, First-Stage Rotor Blading," NASA TP-1493, Aug. 1979.

8 Crouse, J. E., and Gorrell, W. T., "Computer Program for Aerodynamic and Blading Design for Multistage Axial-Flow Compressors." Proposed NASA TP.

9 Katsanis, T., "Fortran Program for Calculating Transonic Velocities on a Blade-To-Blade Stream Surface of a Turbomachine," NASA TN D-5427, 1969.

10 McNally, W. D., "Fortran Program for Calculating Compressible Laminar and Turbulent Boundary Layers in Arbitrary Pressure Gradients," NASA TN D-5681, 1970.

11 Cohen, C. B. and Reshotko, E., "The Compressible Laminar Boundary Layer with Heat Transfer and Arbitrary Pressure Gradient," NACA TR-1294, 1956.

12 Schlicting, H., "Origin of Turbulence II," Boundary-Layer Theory, 7th Ed., McGraw-Hill, New York, 1979, pp. 489-554.

13 Sasman, P. K. and Cresci, R. J. "Compressible Turbulent Boundary Layer with Pressure Gradient and Heat Transfer," AIAA Journal, Vol. 4, No. 1, Jan. 1966, pp. 19-25.

14 Sanger, N. L., "Two-Dimensional Analytical and Experimental Performance Comparison for a Compressor Stator Section with D-Factor of 0.47," NASA TN D-7425, Oct. 1973.

15 Katsanis, T., Unpublished Addendum to Reference 9.

16 Von Doenhoff, A. E. and Tetervin, N., "Determination of General Relations for the Behavior of Turbulent Boundary Layers," NACA Wartime Report L-382, 1943.

17 Preston, J. H , "The Minimum Reynolds Number for a Turbulent Boundary Layer and the Selection of a Transition Device," Journal of Fluid Mechanics, Vol. 3, Pt. 4, Jan. 1958, pp. 373-384.

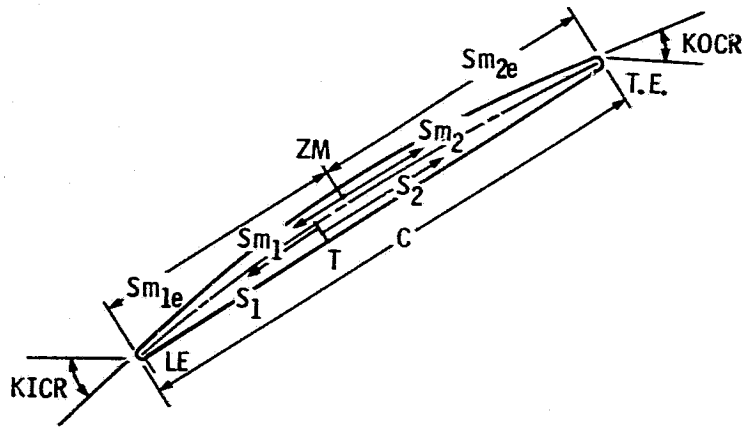

Figure 1. - Blade geometry nomenclature.

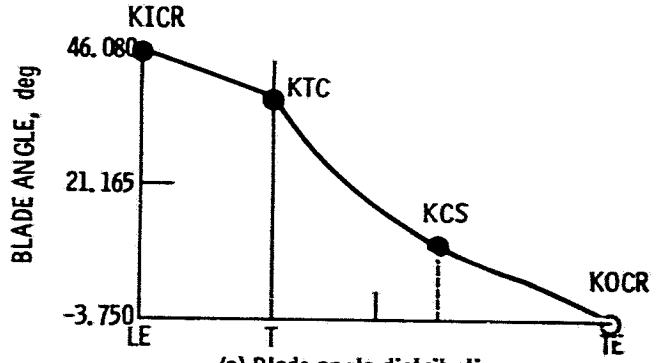

(a) Blade angle distribution.

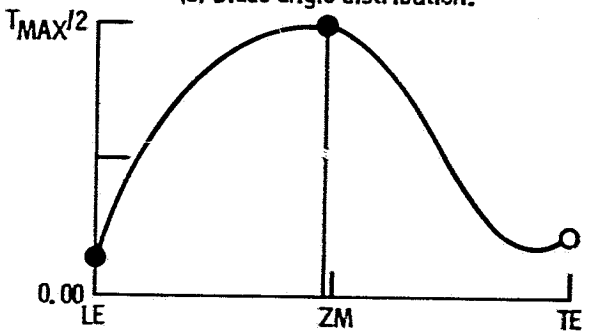

(b) Thickness distribution.

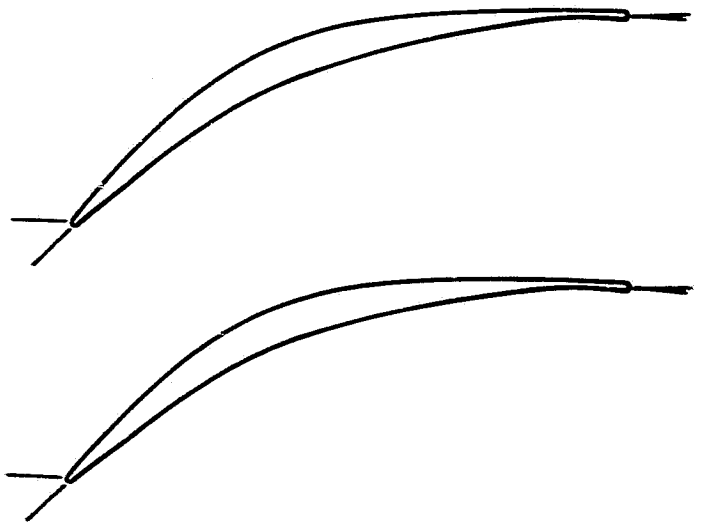

(c) Blade shape.

Figure 2. - Initial blade geometry used in optimization search.

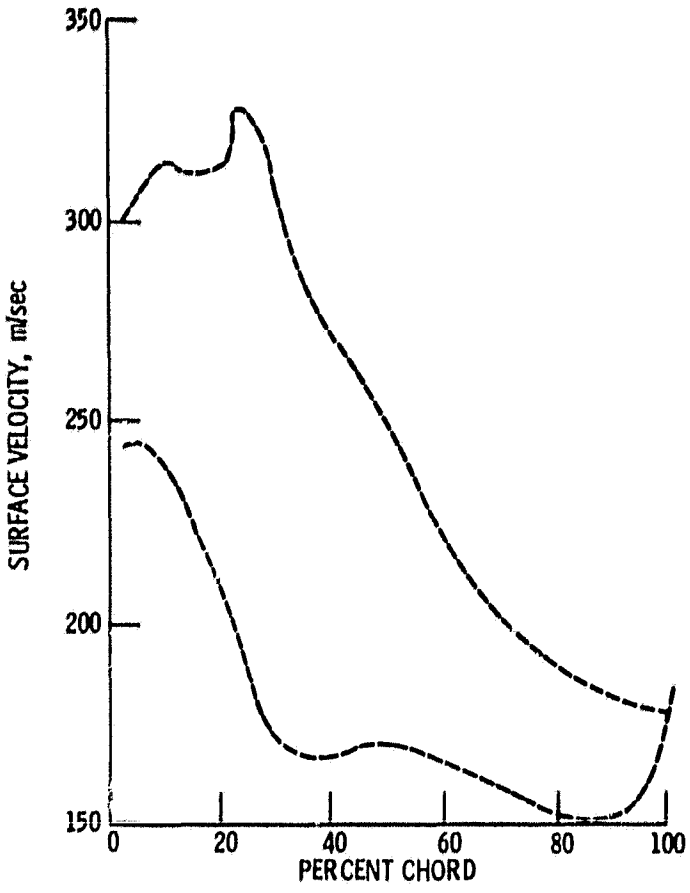

Figure 3. - Initial surface velocity distribution.

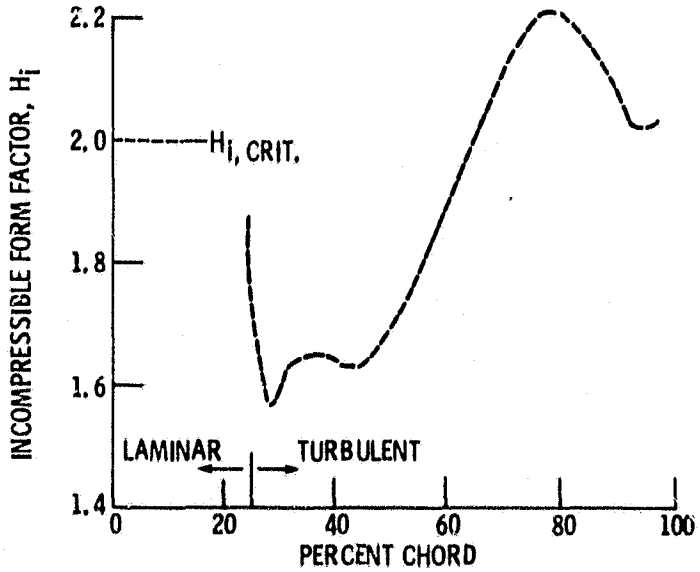

Figure 4. - Initial design-suction surface turbulent boundary layer form factor distribtion.

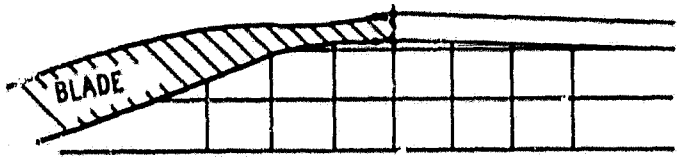

(a) Construction of effective wake.

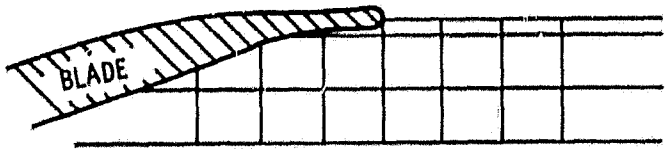

(b) Original trailing edge model (ref. 9).

Figure 5. - Mass flow injection model; TSONIC program.

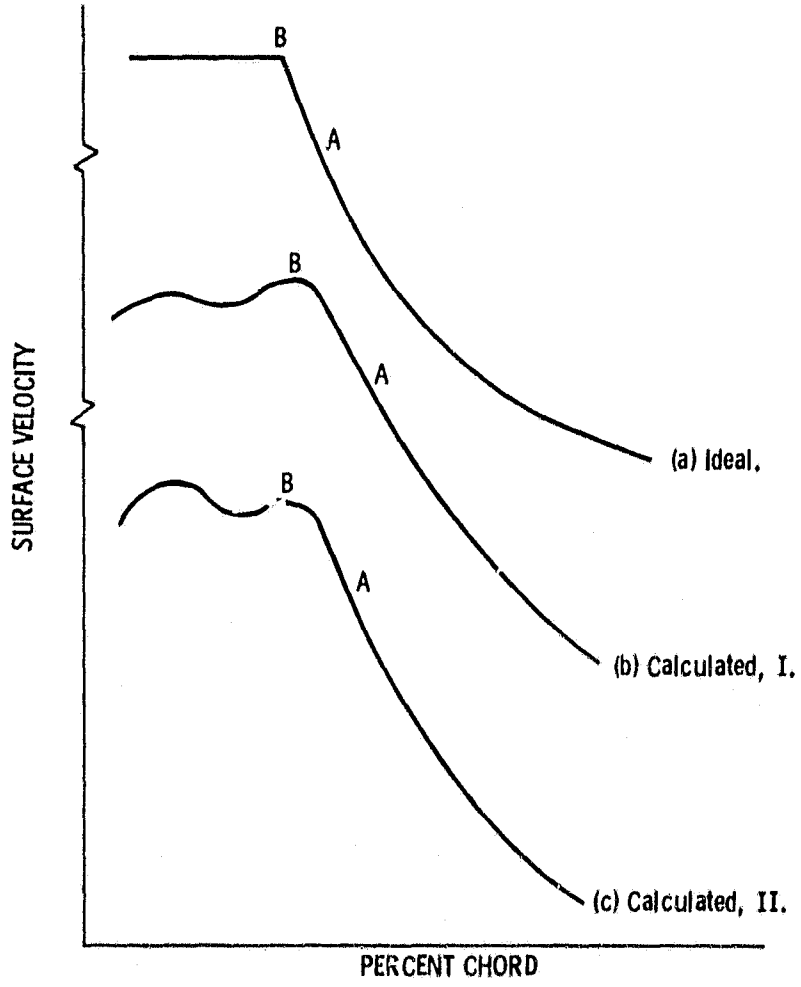

Figure 6. - Representation of ideal and calculated suction surface velocities.

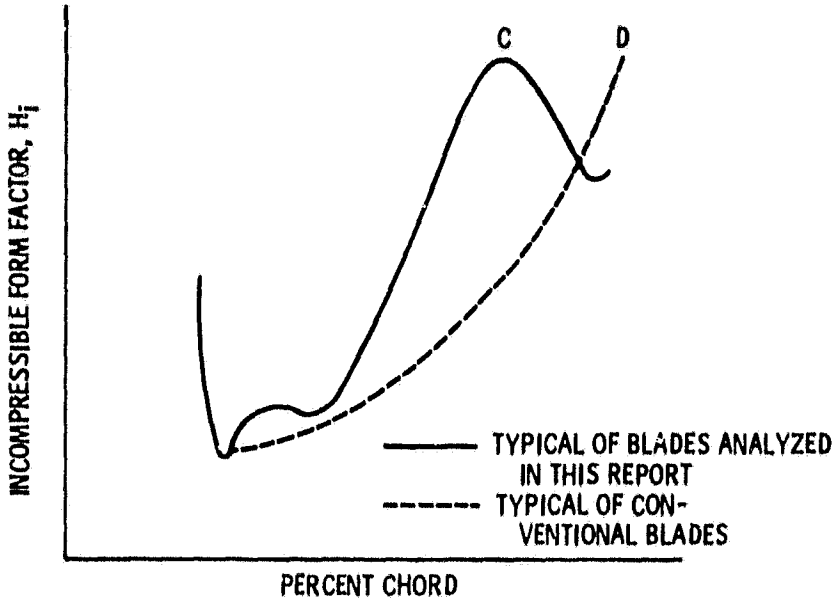

Figure 7. - Turbulent incompressible form factors for different classes of blades.

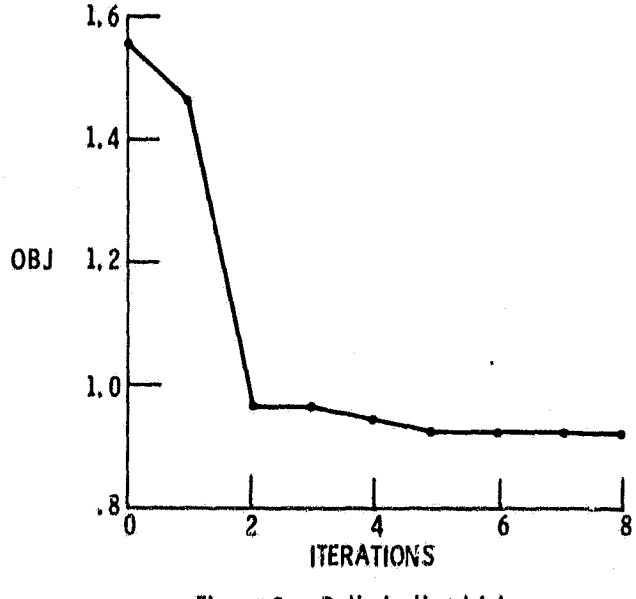

Figure 8. - Optimization history.

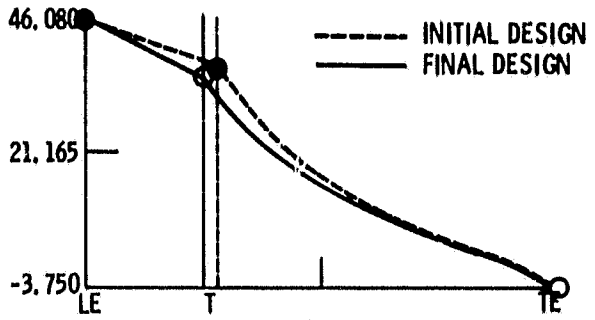

CENTERLINE PATH DISTANCE

(a) Blade angle distribution.

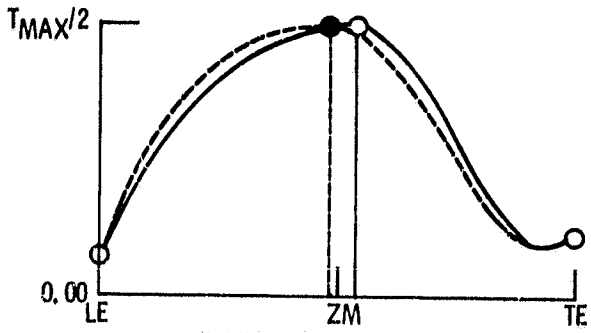

CENTERLINE PATH DISTANCE
ZERO REFERENCE AT MAX THICKNESS POINT

(b) Thickness distribution.

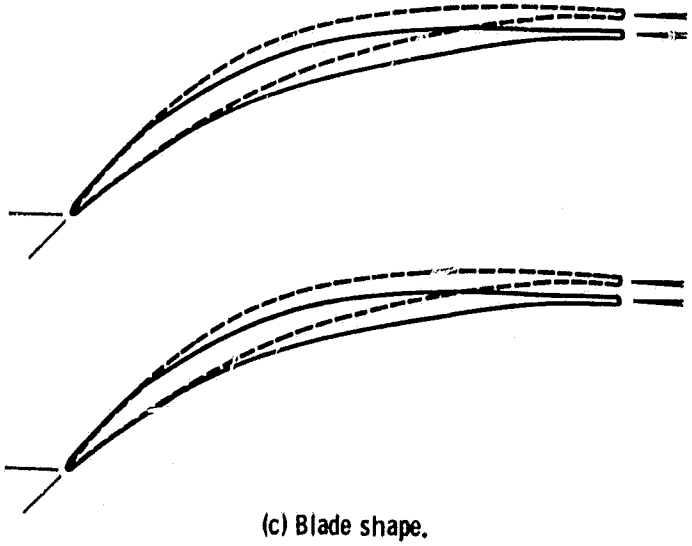

(c) Blade shape.

Figure 9. - Comparisons of initial and final blade designs.

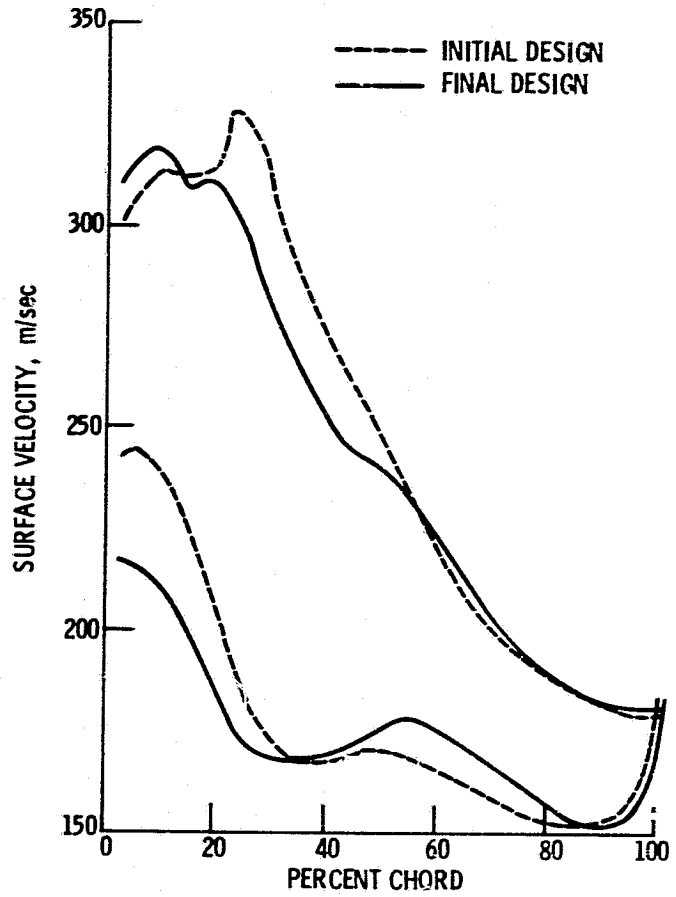

Figure 10. - Comparison of initial and final blade surface velocity distributions.

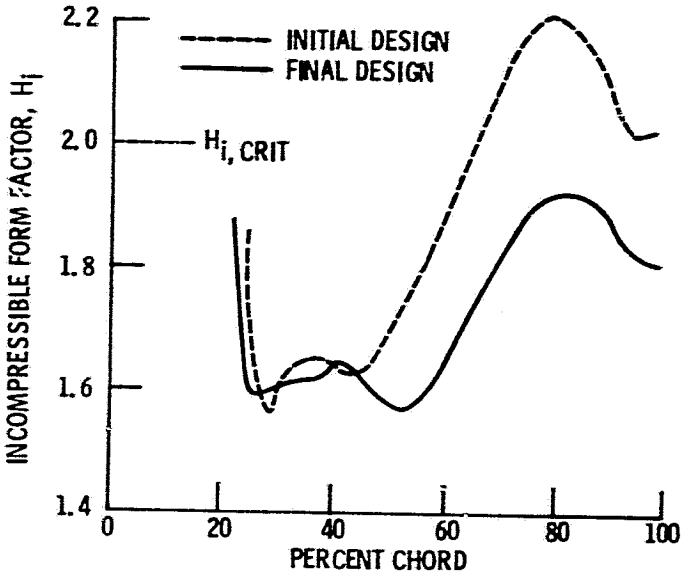

Figure 11. - Comparison of initial and final suction surface turbulent boundary layer incompressible form factor.

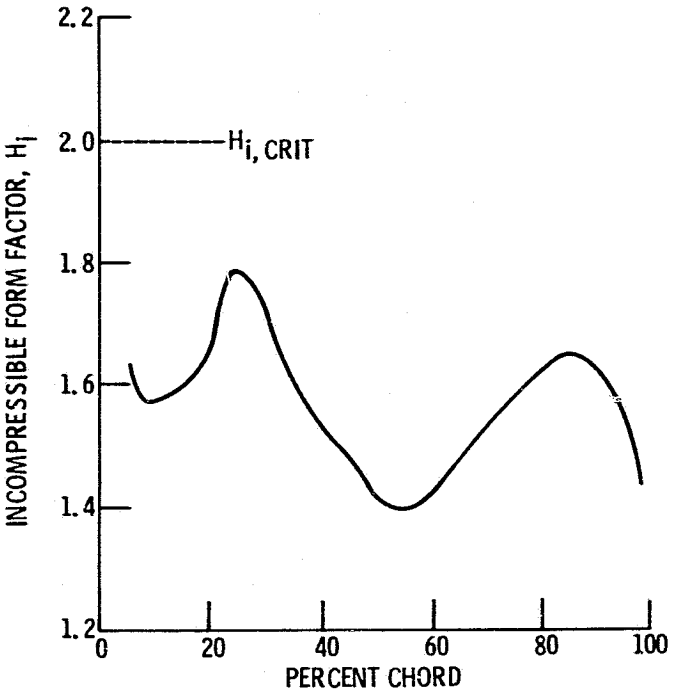

Figure 12. - Final blade design turbulent boundary layer incompressible form factor, pressure surface.

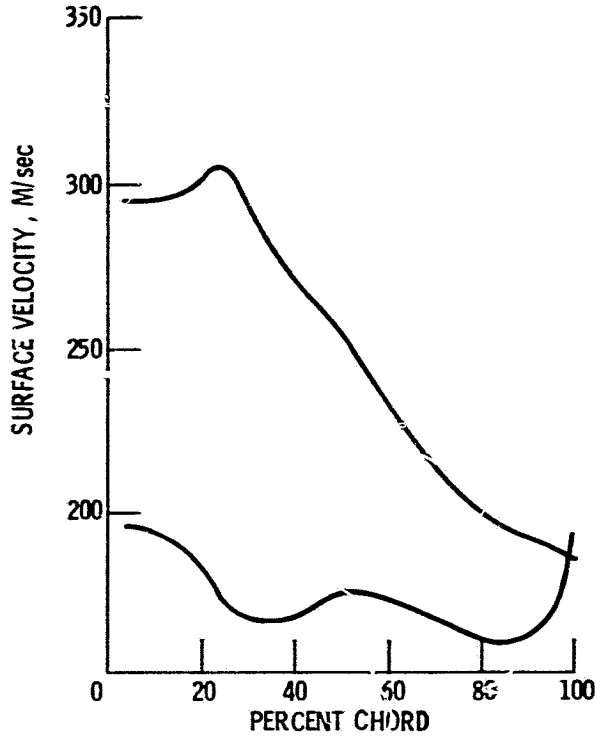

(a) Surface velocity distribution.

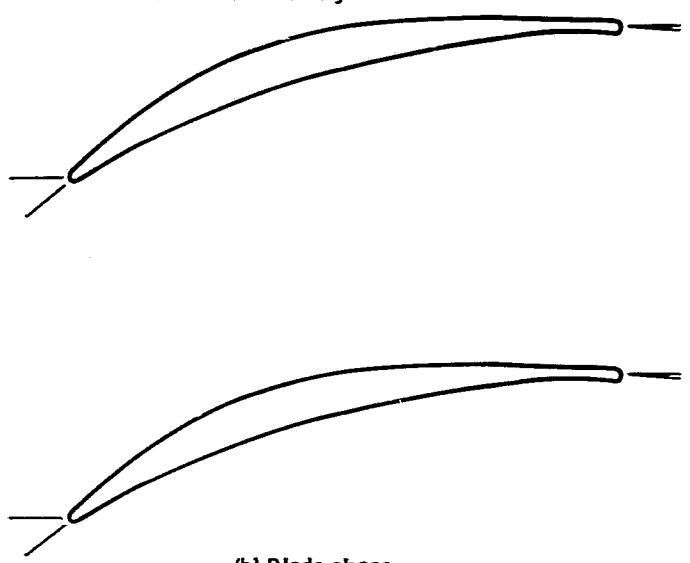

(b) Blade shape.

Figure 13. - Surface velocity distribution and blade shape, final blade, 50 percent span from tip.

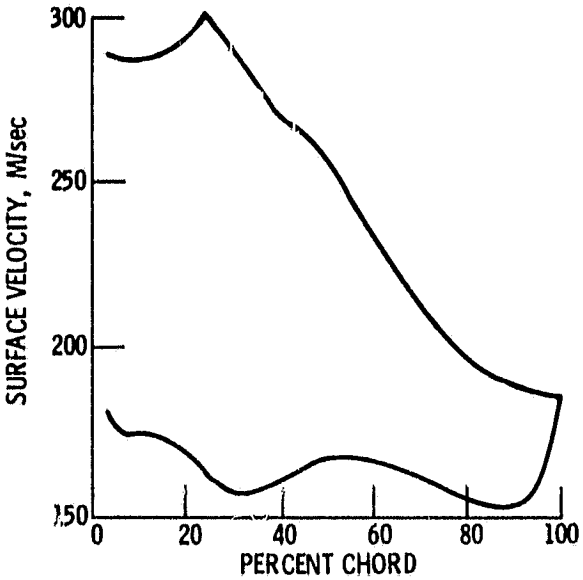

(a) Surface velocity distribution.

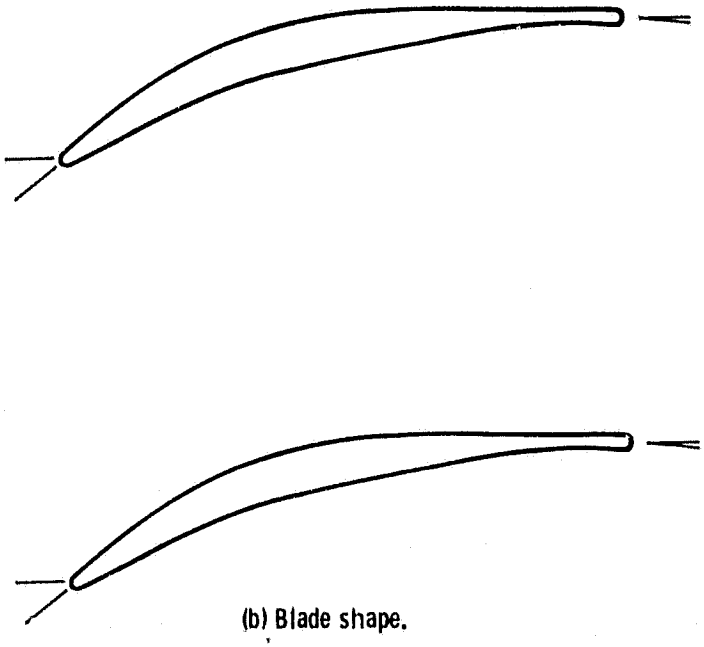

(b) Blade shape.

Figure 14. - Surface velocity distribution and blade shape, final blade, 10 percent span from tip.